



## ARTICLE

# Population pharmacokinetic analyses for belzutifan to inform dosing considerations and labeling

Dhananjay D. Marathe<sup>1,\*</sup>  | Petra M. Jauslin<sup>2</sup> | Huub Jan Kleijn<sup>2</sup> |  
 Carolina de Miranda Silva<sup>1</sup> | Anne Chain<sup>1</sup> | Thomas Bateman<sup>1</sup> | Peter M. Shaw<sup>1</sup> |  
 Anson K. Abraham<sup>1,\*</sup>  | Eunkyung A. Kauh<sup>1</sup> | Yanfang Liu<sup>1</sup> | Rodolfo F. Perini<sup>1</sup> |  
 Dinesh P. de Alwis<sup>1,\*</sup> | Lokesh Jain<sup>1,\*</sup>

<sup>1</sup>Merck & Co., Inc., Rahway,  
New Jersey, USA

<sup>2</sup>Certara Strategic Consulting,  
Princeton, New Jersey, USA

## Correspondence

Anne Chain, Merck & Co., Inc.,  
Rahway, NJ, USA.

Email: [anne.chain@merck.com](mailto:anne.chain@merck.com)

## Funding information

Merck Sharp & Dohme LLC, a  
subsidiary of Merck & Co., Inc.,  
Rahway, NJ, USA

## Abstract

Belzutifan (Welireg, Merck & Co., Inc., Rahway, NJ, USA) is an oral, potent inhibitor of hypoxia-inducible factor 2 $\alpha$ , approved for the treatment of certain patients with von Hippel–Lindau (VHL) disease-associated renal cell carcinoma (RCC), central nervous system hemangioblastomas, and pancreatic neuroendocrine tumors. It is primarily metabolized by the polymorphic uridine 5'-diphospho-glucuronosyltransferase (UGT) 2B17 and cytochrome (CYP) 2C19. A population pharmacokinetic (PK) model was built, using NONMEM version 7.3, based on demographics/PK data from three clinical pharmacology (food effect, formulation bridging, and genotype/race effect) and two clinical studies (phase I dose escalation/expansion in patients with RCC and other solid tumors; phase II in patients with VHL). Median (range) age for the combined studies was 55 years (19–84) and body weight was 73.6 kg (42.1–165.8). Belzutifan plasma PK was well-characterized by a linear two-compartment model with first-order absorption and elimination. For patients with VHL, the predicted geometric mean (% coefficient of variation) apparent clearance was 7.3 L/h (51%), apparent total volume of distribution was 130 L (35%), and half-life was 12.39 h (42%). There were no clinically relevant differences in belzutifan PK based on the individual covariates of age, sex, ethnicity, race, body weight, mild/moderate renal impairment, or mild hepatic impairment. In this model, dual UGT2B17 and CYP2C19 poor metabolizers (PMs) were estimated to have a 3.2-fold higher area under the plasma concentration-time curve compared to UGT2B17 extensive metabolizer and CYP2C19 non-PM patients. This population PK analysis enabled an integrated assessment of PK characteristics with covariate effects in the overall population and subpopulations for belzutifan labeling.

\*These authors were employees of Merck Sharp & Dohme LLC, a subsidiary of Merck & Co., Inc., Rahway, NJ, USA at the time of study.

This is an open access article under the terms of the [Creative Commons Attribution-NonCommercial-NoDerivs](https://creativecommons.org/licenses/by-nc-nd/4.0/) License, which permits use and distribution in any medium, provided the original work is properly cited, the use is non-commercial and no modifications or adaptations are made.

© 2023 Merck Sharp & Dohme LLC. *CPT: Pharmacometrics & Systems Pharmacology* published by Wiley Periodicals LLC on behalf of American Society for Clinical Pharmacology and Therapeutics.

## Study Highlights

### WHAT IS THE CURRENT KNOWLEDGE ON THE TOPIC?

Belzutifan is a hypoxia-inducible factor inhibitor recently approved by the US Food and Drug Administration (FDA) for treatment of adult patients with von Hippel–Lindau (VHL) disease who require therapy for associated renal cell carcinoma (RCC), central nervous system hemangioblastomas, or pancreatic neuroendocrine tumors, not requiring immediate surgery. There are currently no publications reporting a comprehensive PK analysis of belzutifan.

### WHAT QUESTIONS DOES THIS STUDY ADDRESS?

This study provides a comprehensive analysis of the pharmacokinetic (PK) profile of belzutifan describing its population PK using phase I data in healthy participants; phase I data in patients with advanced RCC and solid tumors; and phase II data in patients with VHL RCC. The analysis was aimed at determining the impact of intrinsic/extrinsic factors, including body weight, food, formulation, UGT2B17 and/or CYP2C19 phenotype, and delayed dosing on PK characteristics of belzutifan in the patient population, and to investigate a possible need for dose adjustment based on demographic and genetic patient factors.

### WHAT DOES THIS STUDY ADD TO OUR KNOWLEDGE?

This study demonstrated that no dose adjustment from the recommended 120-mg q.d. dose is necessary based on body weight, age, fed or fasted state, or delayed dosing. The UGT2B17/CYP2C19 dual poor metabolizer (PM) phenotype shows a potential for higher belzutifan exposure (area under the plasma concentration-time curve) compared to the reference group; therefore, whereas the starting dose is the same, it is advised to closely monitor such patients for adverse reactions. Of note, in the overall US population, the expected frequency of the UGT2B17/CYP2C19 dual PM phenotype is estimated to be ~0.5%, whereas in East Asians, the frequency can reach 15%.

### HOW MIGHT THIS CHANGE DRUG DISCOVERY, DEVELOPMENT, AND/OR THERAPEUTICS?

This report helps to inform belzutifan PK characteristics and dosing for patients and prescribers. It informs PK parameter estimates for the relevant clinical population and the final formulation, as well as suitable dosing recommendations for labeling.

## INTRODUCTION

Von Hippel–Lindau (VHL) disease is a hereditary syndrome transmitted in an autosomal dominant manner, in which the VHL protein is lost or functionally compromised due to a germline mutation or deletion of the *VHL* gene.<sup>1</sup> Affected individuals are at risk for the development of vascular tumors in a number of organs, including the kidneys, central nervous system (CNS), pancreas, and adrenal glands. In ~70% of patients with VHL disease-associated renal cell carcinoma (VHL-RCC), the disease is the clear cell RCC (ccRCC) histological subtype, representing a leading cause of mortality. Loss of the VHL protein or its function is the cause of most hereditary and sporadic cases of ccRCC.<sup>2</sup> The VHL protein binds to and promotes the degradation of hypoxia-inducible factor

(HIF)-2 $\alpha$ , a transcription factor and regulator of oxygen homeostasis.<sup>1</sup> Activation of HIF-2 $\alpha$  has been found to correlate with disease development across benign and malignant VHL disease-associated tumors.<sup>3</sup>

Belzutifan (Welireg, Merck & Co., Inc., Rahway, NJ, USA) is a potent and selective oral inhibitor of HIF-2 $\alpha$  both in vitro and in vivo. Nonclinical pharmacology studies have confirmed the specificity and selectivity of belzutifan for HIF-2 $\alpha$  and demonstrated antitumor activity in mouse VHL-deficient tumor xenograft models of ccRCC.<sup>4</sup> Belzutifan is approved in the United States for treatment of adult patients with VHL disease who require therapy for associated RCC, CNS hemangioblastomas, or pancreatic neuroendocrine tumors, not requiring immediate surgery.

The belzutifan clinical pharmacology development program evaluated the pharmacokinetics (PK) and

pharmacodynamics of belzutifan in patients with VHL-RCC and advanced solid tumors, and in healthy participants. Two formulations were used in the clinical pharmacology development program: an oral compressed fit-for-purpose (FFP) tablet, and a film-coated tablet, the final market formulation (FMF).

In vitro data and pharmacogenetic evaluations in a clinical study (MK-6482-007) suggest that metabolism of belzutifan is primarily via uridine 5'-diphospho-glucuronosyltransferase (UGT) 2B17 and cytochrome (CYP) 2C19 enzymes. Both of these are polymorphic enzymes with various phenotypes ranging from ultra-rapid metabolizers, extensive metabolizers (EMs), and intermediate metabolizers (IMs) to poor metabolizers (PMs) that have no enzyme activity. Urinary excretion was found to be a minor pathway for elimination of belzutifan ( $\leq 4\%$  of dose) for rats, dogs, and monkeys.

This paper describes the population PK analysis of belzutifan using phase I data in healthy participants (Studies NCT03445169, MK-6482-006, and MK-6482-007), phase I data in patients with RCC and other solid tumors (ST; Study NCT02974738) and phase II data in patients with VHL-RCC (Study NCT03401788). The analysis was aimed at characterizing the impact of intrinsic/extrinsic factors on belzutifan PK in the patient population to support the benefit-risk assessment and dose justification, as well as to support regulatory filing and product labeling.

## METHODS

### Study design

The population PK model was developed using data from 4 phase I studies and one pivotal phase II study listed in Table 1. All studies except for Study 1 and Study 4 were completed at the time of analysis. The data cutoff used for the latter two studies was June 1, 2020. The final population PK dataset included plasma concentration data from 239 participants, including 61 patients with VHL-RCC and 95 patients with advanced RCC or ST.

For the population PK analysis, an individual was defined as evaluable if both of the following criteria were satisfied: received at least one dose of belzutifan and had at least one measurable belzutifan concentration with associated sampling time and dosing information.

### Population PK model development

The population PK analysis was performed using a nonlinear mixed effects modeling approach. This approach estimated the typical values of parameters as well as their

interindividual variability (IIV). Linear one-, two-, and three-compartment models were evaluated depending on the shape of the observed concentration-time profiles. Absorption was modeled as a first-order process with lag time.

Additive, log-additive, proportional and additive + proportional error models were explored for residual variability.

Exponential error models were used to describe IIV in the PK parameters, assuming log-normal parameter distribution. IIV was introduced and retained if inclusion did not cause model instability, and if estimates were not close to zero. As a start, a diagonal  $\Omega$ -structure was used. The inclusion of off-diagonal elements was investigated.

Goodness-of-fit and appropriateness of the random effect models were assessed by means of diagnostic plots.

### Covariates

Covariates were identified using a stepwise selection procedure as implemented in the stepwise covariate model (SCM) tool of Perl speaks NONMEM (PsN)<sup>5</sup> with testing of linear and nonlinear relationships in a forward inclusion ( $\Delta$  objective function value [OFV] of 6.63,  $p < 0.01$  for 1 degree of freedom [DF]) and backward exclusion ( $\Delta$ OFV of 10.8,  $p < 0.001$  for 1 DF) procedure. The resulting final model only contained covariates that met the predefined statistical criteria. The clinical relevance of any relationship was also considered.

Categorical covariates were only tested if at least 5% of participants (or 10 participants, whichever was smaller) belonged to that category. Categories with low sample-sizes were pooled when needed to improve the power of the assessment.

Covariates investigated included age, body weight, body mass index (BMI), sex, race, ethnicity, formulation, fed versus fasted dosing, disease status, National Cancer Institute (NCI) index (composite of aspartate aminotransferase and total bilirubin; for hepatic impairment evaluation), eGFR (for renal impairment evaluation), and UGT2B17 and CYP2C19 phenotypes.

### Model evaluation

A nonparametric bootstrap analysis<sup>6</sup> was conducted to evaluate the stability of the final model and to estimate confidence intervals (CIs) for the model parameters. The bootstrap analysis was performed with 1000 replicates of the dataset, generated by random resampling of subjects from the original dataset with replacement, stratified by study.

**TABLE 1** Summary of studies included in population PK analyses.

Study no.	Description	N	Formulation	Doses	Population	Belzutifan PK Assessments
Study 1 (NCT02974738)	Ph I dose-escalation/ expansion	95 Escalation: N = 43 (22 RCC and 21 ST); Expansion: N = 52 (all RCC)	FFP	Escalation: 20, 40, 80, 120, 160, and 240 mg q.d. (N = 6–7 each), 120 mg b.i.d. (N = 6) Expansion: 120 mg q.d.	ST/RCC	Plasma concentrations were measured at weeks 1 and 3 (1 h predose and 0.5, 1, 1.5, 2, 4, 6, 8, 12 and 24 h postdose). Trough samples were measured at weeks 2, 4, 5, 7, and 9. One sample each at week 13 and 17 was collected with no drug administration
Study 2 (NCT03445169)	Ph I food-effect	16	FFP	120 mg SD fed and fasted	HP	Plasma concentrations were measured predose and 0.5, 1, 1.5, 2, 4, 6, 9, 12, 18, 24, 36, 48, 60, 72, 96, 120, 144, 168, and 192 h postdose
Study 4 (NCT03401788)	Ph II single arm	61	Patients were switched from FFP to FMF	120 mg q.d.	VHL-RCC	Plasma concentrations were measured at weeks 1 and 3 (predose and 2 and 5 h postdose). Trough samples were collected at weeks 5, 9, and 13 and additional trough samples were available in a subset of patients
Study 6 PT2977-104/ MK-6482-006	Ph I cross-over relative bioavailability	18	FFP vs. FMF	120 mg SD FFP 120 and 200 mg SD FMF	HP	Plasma concentrations were measured predose and 0.5, 1, 1.5, 2, 3, 4, 6, 9, 12, 18, 24, 36, 48, 60, 72, 96, and 120 h postdose
Study 7 PT2977-104/ MK-6482-007	Ph I parallel Japan PK (genotype/race effect)	49	FMF	40 mg SD	HP (Japanese and White)	Plasma concentrations were measured predose and 0.5, 1, 1.5, 2, 3, 4, 5, 6, 9, 12, 24, 48, 72, 96, 120, and 168 h postdose after single dose administration. Additional samples were drawn on days 15 and 22

Abbreviations: b.i.d., twice daily; FFP, fit-for-purpose formulation; FMF, final market formulation; HP, healthy participants; Ph, Phase; PK, pharmacokinetics; q.d., once daily; RCC, (advanced) renal cell carcinoma; SD, single dose; ST, solid tumor (advanced, besides RCC); VHL, Von Hippel-Lindau; VHL-RCC, VHL disease-associated RCC.

Visual predictive checks (VPCs) were used to evaluate the predictive ability of the final model<sup>7</sup> and were based on 500 simulations. They were performed with prediction correction<sup>8</sup> and stratified by study. Plots of observed data distributions were compared to simulated distributions to demonstrate the model's ability to adequately predict the data on which the model was based.

## Simulations

The univariate effect of covariates on exposure (AUC at steady-state [AUC<sub>ss</sub>] for 120-mg belzutifan once daily [q.d.]) was simulated by varying one covariate at a time while all other covariates were set to those of a “typical” subject. Exposures at the 5th percentile and the 95th percentile of the observed values of continuous covariates in the study population, and at the different levels of the categorical covariates, were compared with the exposure estimates for the “typical” subject and the range of exposures in the entire study population (all 5 studies pooled and separately for Study 4). The results were illustrated by tornado plots.

Secondary PK parameters at steady-state (SS) such as AUC, maximum plasma concentration ( $C_{\max}$ ), time to  $C_{\max}$  ( $T_{\max}$ ), minimum plasma concentration ( $C_{\min}$ ), effective elimination and absorption half-lives ( $t_{1/2 \text{ eff}}$  and  $t_{1/2 \text{ abs}}$ , respectively) were obtained through simulation. These simulations were based on the patient population in Study 4. Each patient's covariates were used 10 times, creating a dataset consisting of 610 “virtual patients.” 24-h profiles at SS, assuming a dose of 120 mg q.d., were simulated, with observations at 0, 0.5, 1, 1.5, 2, 3, 4, 5, 6, 9, 12, 18, and 24 h postdose. From these, individual secondary PK parameters and summary statistics were calculated. All patients in Study 4 had received the FFP formulation during PK sampling, which was reflected in the covariates in the simulation dataset. However, the simulations were repeated after setting the covariate “formulation” to FMF for all patients, to obtain the same exposure parameters for a (virtual) population receiving the final market formulation in the simulations.

Accumulation ratios were calculated by dividing SS  $C_{\max}$  and  $C_{\min}$  with the respective  $C_{\max}$  and  $C_{\min}$  from a single dose simulation with otherwise identical settings. To determine time to SS, 120-mg doses for 7 consecutive days were simulated, with observations at 0, 0.5, 1, 1.5, 2, 3, 4, 5, 6, 8, 12, 15, 18, and 24 h after each dose. SS was assumed to be reached when  $C_{\min}$  changed less than 5% in two consecutive dosing intervals.

Delayed dose scenarios were simulated to assess the impact of missed and delayed doses, including a delay in second q.d. dose of 12, 16, 18, or 21 h.

## Software

Assembly of the population PK dataset was performed using SAS, version 9.4. NONMEM, version 7.3 (ICON) was used for the population PK analysis. Model fitting was performed on a grid of CentOS 7.1 Linux servers with Intel FORTRAN Compiler for Linux, version 12.0.4 (Intel Corporation). The PsN version 4.8.1 ([psn.sourceforge.net](http://psn.sourceforge.net)) and R version 4.0.0 were used for the exploratory analysis and post-processing of NONMEM output.

## RESULTS

### Data

The full PK analysis dataset included 5291 measurable PK observations from 239 participants. One patient in Study 1 was excluded because no postdose observations were available. Seven observations were excluded: one because of missing sampling time, and six deemed as outliers based on predefined criteria (e.g., rising concentration without recorded dose administration, or unrealistic concentrations >3 times all other samples for the respective individual).

### Base model

Linear one-, two-, and three-compartment structural models with first-order elimination were tested. The two-compartment structure provided the best fit to the data, and a third compartment did not further improve the model fit. Absorption was described by a first-order process with lag time. A body weight effect on clearances and volumes (V), and a food effect on the absorption rate constant (KA) were included in the base model as structural covariates to obtain an acceptable model fit.

IIV was evaluated on all parameters and retained on KA, CL, central (V2), and peripheral volume of distribution (V3), with an  $\Omega$ -block for CL-V2-V3. The proportional error model was selected from the different residual error models evaluated.

The parameter estimates for the base model are presented in Table S1. All parameters were estimated with good precision. The  $\eta$ -shrinkage for the base model was low for apparent clearance (CL/F; 0.58%) and acceptable for apparent central volume of distribution (V2/F; 24%) and apparent peripheral volume of distribution (V3/F; 27%). The  $\epsilon$ -shrinkage was low (5.2%). The goodness-of-fit (GOF) plots for the base model are shown in Figure S1.



## Covariate selection

In addition to the body weight effect on CL/F and volumes and the food effect on KA, the following covariates were included in the SCM: age, sex, race, ethnicity, disease status, hepatic dysfunction, eGFR, UGT2B17 phenotype and CYP2C19 phenotype on CL/F; age, sex, race, ethnicity, disease status on V2/F; formulation on KA; formulation and food effect on lag time; and UGT2B17 phenotype and CYP2C19 phenotype on bioavailability (F). BMI was not tested, because it is correlated with body weight, which was already included in the base model. Patient demographics pooled for all studies are shown in [Table S2](#). The final SCM results are shown in [Table S3](#).

The sex effect on V2/F was further investigated, because the studies were unbalanced with respect to this covariate: the single-dose healthy participant studies (2, 6 and 7) enrolled no male participants (Studies 2, 7) or very few male participants (Study 6,  $N=3$ ). In contrast, in the multiple dose studies in patients, the majority of patients were men. It is therefore possible that the identified sex effect may represent a population or study effect. Exploratory boxplots of  $\eta$ s by sex show no indication of a possible influence (data not shown). Therefore, the SCM was repeated without the covariate “sex.” No additional covariate was identified in its place.

## Final population PK model

Covariates identified by the SCM procedure were manually introduced individually to ensure successful termination of runs and avoid over-parameterization. CYP2C19 categories were merged, as only the PM category had a significantly different CL/F compared to all other categories. Although the data supported a different CL/F for all three UGT2B17 categories, only two categories could be maintained with regard to the effect on F (EMs and IMs merged). The food effect on lag time could not be included, as the respective coefficient could not be estimated with sufficient precision (CI included 0), and the run terminated with rounding errors. The sex effect on V2/F was not included in the final model (as discussed above). The structure of the variance–covariance matrix and the residual error structure were defined after covariate inclusion.

No effects of renal and hepatic impairment were found in the covariate analysis based on available data. The effects of severe renal impairment and moderate or severe hepatic impairment could not be evaluated, as no or too few participants with the conditions were included in the studies. To further illustrate the relationship between the respective impairment status and belzutifan exposure, individual CL/F

or AUC<sub>ss</sub> by renal and hepatic impairment category after inclusion of all covariates are shown in [Figure S2](#).

The parameter estimates for the final population PK model are presented in [Table 2](#). Unexplained IIV (% coefficient of variation [CV]) for CL/F was reduced by 14% compared to the base model. GOF plots for the final population PK model were unbiased ([Figure S1](#)). Overall,  $\eta$ -distributions were close to normal (with heavier tails for KA), reflecting the adequacy of the exponential models for IIV. Conditional weighted residuals in all studies also approximately followed a normal distribution.

Effect sizes of continuous covariates are summarized in [Table S4](#). The effects of the continuous covariates body weight and age appear to be moderate in size. The largest effect in this group of covariates is the body weight effect on distribution volumes for the heaviest patients (+65% in V2/F and V3/F for the 95% body weight percentile). CL/F and apparent inter-compartmental clearance (Q/F) were scaled by the same estimated exponent, as were V2/F and V3/F.

Effect sizes of categorical covariates are shown in [Table 3](#). Both food and formulation have a considerable impact on KA (−88% in fed condition compared to fasted, −47% with FMF compared to FFP). UGT2B17 and CYP2C19 phenotypes have a moderate impact on CL/F (<±40%), and the direct effect of UGT2B17 phenotype on F is small (11% higher for PMs compared to IMs and EMs).

## Model qualification

A prediction-corrected VPC for the population PK model was performed using optimized binning for each study ([Figure 1](#)). It was based on 500 simulations and stratified by study. The final population PK model was able to predict the observed median and 5th and 95th percentile of observed belzutifan concentrations with good accuracy for Studies 1, 2, 4, and 6. In Study 7, the median concentration and 95th percentile were well captured; however, the lowest concentrations (5th percentile) were underpredicted by the model.

The final population PK model for belzutifan was fitted to 1000 bootstrap replicate datasets, stratified by study, to evaluate model stability and performance. Of these, 351 runs did not terminate successfully, and four runs had estimates near a boundary. Bootstrap statistics were therefore derived from 645 runs. [Table S5](#) compares final model estimates and CIs with the respective estimates obtained by the bootstrap analysis.

## Simulations

The isolated influence of each statistically significant covariate on the exposure of belzutifan after treatment with

**TABLE 2** Final model parameter estimates for belzutifan PK.

Parameter	Estimate	% Relative SE	Asymptotic 95% CI	% Shrinkage
Fixed effects				
CL/F (L/h)	5.63	3.40	5.25; 6.00	–
V2/F (L)	85.4	2.9	80.55; 90.26	–
Q/F (L/h)	5.37	14.07	3.89; 6.85	–
V3/F (L)	30.38	6.65	26.42; 34.34	–
KA (/h)	2.40	7.70	2.04; 2.76	–
ALAG (h)	0.16	1.50	0.16; 0.17	–
KA-FED	–0.88	7.20	–1.00; –0.75	–
CL-WT	0.65	15.55	0.45; 0.84	–
V-WT	1.06	3.99	0.98; 1.14	–
CL-UGT2B17 extensive metabolizers	0.39	19.17	0.24; 0.54	–
CL-UGT2B17 poor metabolizers	–0.24	19.54	–0.34; –0.15	–
CL-CYP2C19 poor metabolizers	–0.36	14.96	–0.47; –0.25	–
F-UGT2B17 poor metabolizers	0.11	22.78	0.061; 0.16	–
KA-FORM	–0.47	34.48	–0.79; –0.15	–
V-AGE	–0.20	23.82	–0.30; –0.11	–
CL-AGE	–0.36	22.57	–0.52; –0.20	–
Random effects				
IIV on CL/F	0.15	11.43	0.11; 0.18	1.6
IIV on V2/F	0.013	24.92	0.0064; 0.019	34
IIV on V3/F	0.19	37.21	0.052; 0.33	32
IIV on KA	1.15	16.38	0.78; 1.52	18
Residual error				
RES HV	0.26	4.77	0.24; 0.28	–
RES PAT	0.29	3.29	0.27; 0.31	–
EPS	1 FIX	0	–	5.2

Note: The following  $\eta$ -correlations were estimated: CL/F-V2/F: 0.40; CL/F-V3/F: 0.54; V2/F-V3/F: 0.38. Equations for the PK parameters were as follows:

$CL/F = CL/F_{pop} * (WT/73.64)^{CL-WT} * (1 + CL-UGT2B17P) * (1 + CL-CYP2C19P) * (AGE/55)^{CL-AGE} * \eta_1$ .

$V2/F = V2/F_{pop} * (WT/73.64)^{V-WT} * (AGE/55)^{V-AGE} * \eta_2$ .

$Q/F = Q/F_{pop} * (WT/73.64)^{CL-WT}$ .

$V3/F = V3/F_{pop} * (WT/73.64)^{V-WT} * \eta_3$ .

$F = 1 * (1 + F-UGT2B17P)$ .

$KA = KA_{pop} * (1 + KA-FED) * (1 + KA-FORM) * \eta_4$ .

Abbreviations: ALAG, lag time; CI, confidence interval; CL, clearance; CL-AGE, age effect on CL (exponent); CL/F, apparent clearance; CL-CYP2C19, CYP2C19 phenotype effect on CL (coefficient); CL-UGT2B17, UGT2B17 phenotype effect on CL (coefficient); CL-WT, body weight effect on clearances (exponent); CV, coefficient of variation; EPS,  $\epsilon$  (random error); F, bioavailability; F-UGT2B17, UGT2B17 phenotype effect on F (coefficient); HV, healthy volunteer; IIV, interindividual variability; KA, absorption rate constant; KA-FED, food effect on KA (coefficient); KA-FORM, formulation effect on KA (coefficient); PAT, patient; PK, pharmacokinetics; pop, population; Q/F, apparent inter-compartmental clearance; RES, proportional residual error; SE, standard error; V2/F, apparent central volume of distribution; V3/F, apparent peripheral volume of distribution; V-AGE, age effect on central volume of distribution (exponent); V-WT, body weight effect on distribution volumes (exponent); WT, body weight;  $\eta$ , difference between population and individual parameter.

120 mg q.d. was evaluated. The effect on exposure was calculated for each covariate individually, with all other covariates fixed to their typical values (as estimated for the reference subject). Continuous covariates were evaluated at the 5th and 95th percentiles of the Study 4 population. Categorical covariate effects were evaluated for each

level. A tornado plot of the effects of significant covariates on belzutifan  $AUC_{ss}$  is shown in Figure 2. Prediction intervals for each of the covariates were within the observed clinical range (90% prediction interval for Study 4).

A comparison of primary and secondary PK parameters obtained by univariate simulation for different UGT2B17

Parameter	Covariate	Absolute parameter value	% Change
KA	Food (fasted)	2.40	0 (reference)
KA	Food (fed)	0.30	−87.6
KA	Formulation (FFP)	2.40	0 (reference)
KA	Formulation (FMF)	1.26	−47.4
CL/F	UGT2B17 (intermediate)	5.63	0 (reference)
CL/F	UGT2B17 (extensive)	7.83	+39.1
CL/F	UGT2B17 (poor)	4.27	−24.2
CL/F	CYP2C19 (extensive)	5.63	0 (reference)
CL/F	CYP2C19 (poor)	3.60	−36.0
F	UGT2B17 (intermediate/ extensive)	1	0 (reference)
F	UGT2B17 (poor)	1.11	11.0

Abbreviations: CL/F, apparent clearance; F, relative bioavailability; FFP, fit-for-purpose formulation; FMF, final market formulation; KA, absorption rate constant; PK, pharmacokinetics.

**TABLE 3** Categorical covariate effects on belzutifan PK parameters.

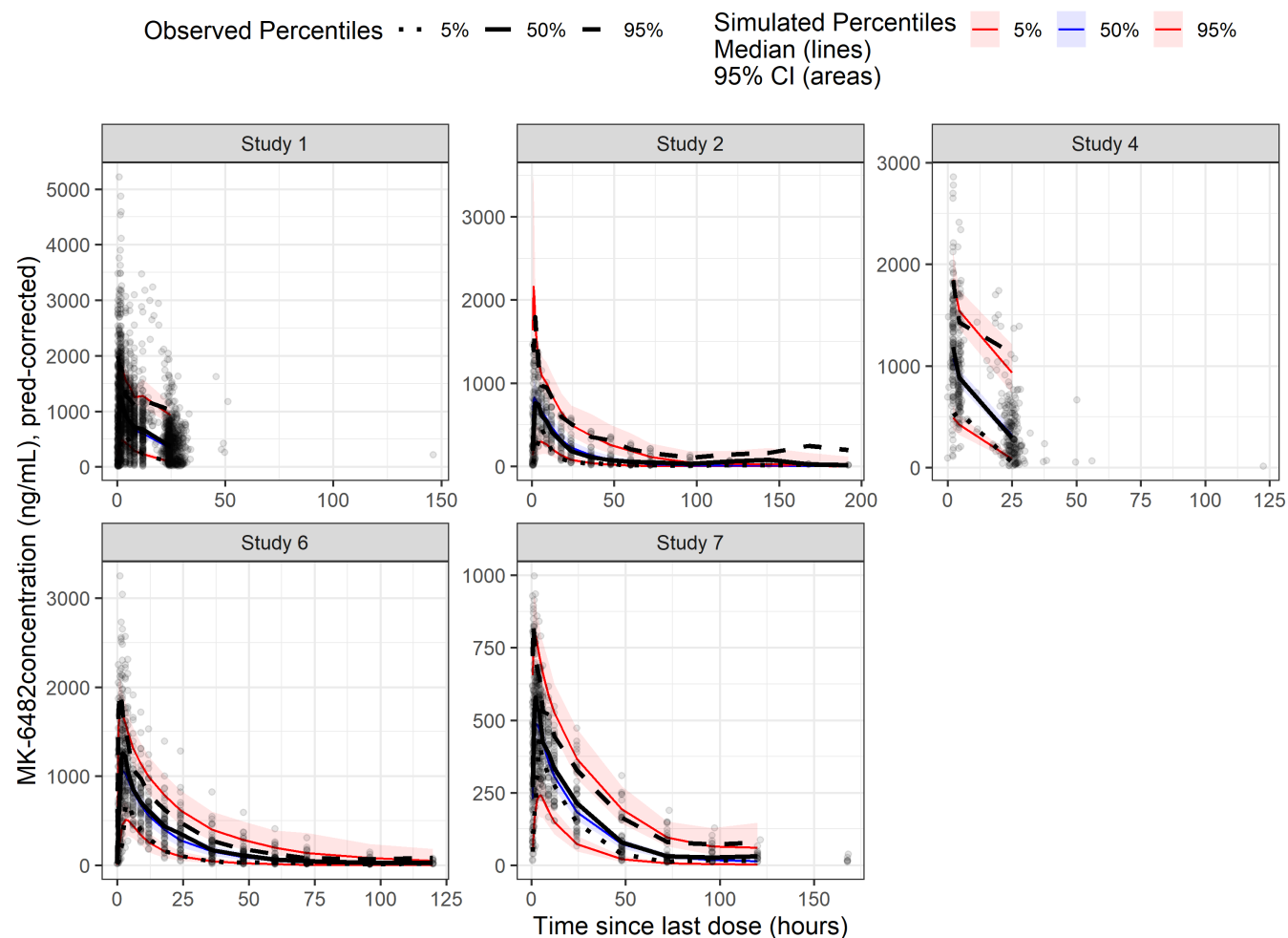


**FIGURE 1** Prediction-corrected VPC by study. A prediction-corrected VPC for the population PK model was performed using optimized binning for each study. Prediction correction was applied to account for differences in dose regimens between patients. CI, confidence interval; PK, pharmacokinetic; VPC, visual predictive check.



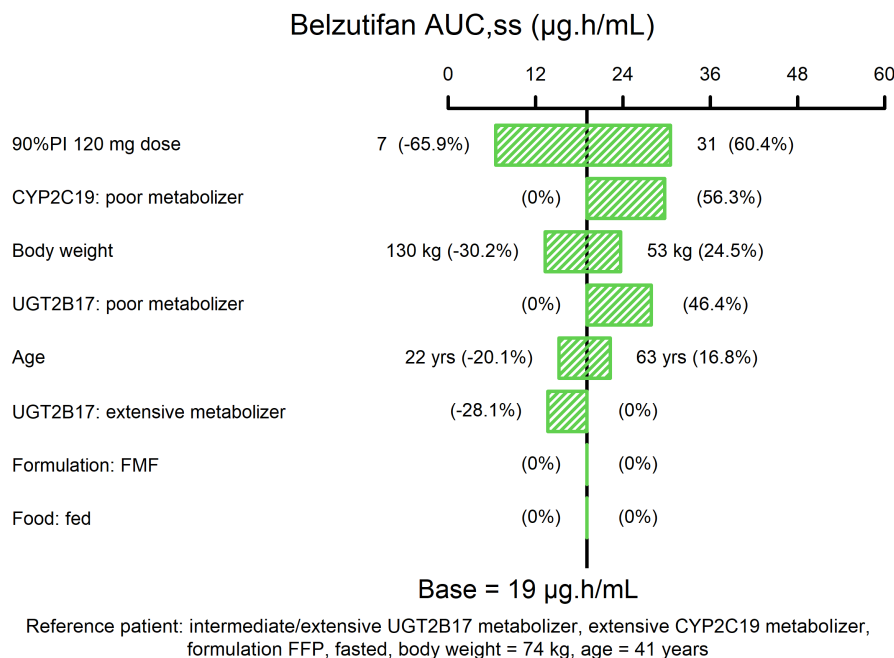


**FIGURE 2** Univariate impact of covariates on Belzutifan AUC<sub>ss</sub> (μg.h/mL) (Study 4). Covariate effects were expressed as a percentage change from the typical value of the reference patient (i.e., a “typical” individual with the specified covariates). The category “extensive CYP2C19 metabolizer” includes all non-poor metabolizers (i.e., intermediate to ultra-rapid metabolizers). Extensive/intermediate UGT2B17 metabolizer denotes a patient with intermediate UGT2B17 effect on CL/F and either intermediate or extensive UGT2B17 effect on bioavailability (categories pooled for effect on F). For continuous covariates, green bars represent the range of exposures between the 5th and 95th percentiles of observed covariate values. AUC<sub>ss</sub>, area under the concentration vs time curve at steady-state; CL/F, apparent clearance; CYP2C19; cytochrome (CYP) 2C19; F, bioavailability, FFP, oral compressed fit-for-purpose tablet; FMF, film-coated tablet, the final market formulation; PI, prediction interval; UGT2B17, uridine 5′-diphospho-glucuronosyltransferase (UGT) 2B17.

and CYP2C19 phenotypes is presented in Table 4. These simulated values are compared to AUC<sub>ss</sub> values calculated from post hoc parameters in Studies 1 and 4 (last column to the right).

Derived PK parameters such as AUC<sub>ss</sub>, C<sub>max</sub>, T<sub>max</sub>, C<sub>min</sub>, t<sub>1/2 eff</sub> and t<sub>1/2 abs</sub> were obtained through simulation. These simulations of SS profiles with a 120-mg q.d. dosing regimen were based on the demographics of the 61 patients with VHL-RCC included in Study 4. The resulting geometric mean values and geometric CV, as well as medians and CV, are presented in Table 5. At SS following 120-mg belzutifan q.d., geometric means (%CV) of AUC for a 24-h interval (AUC<sub>0-24h</sub>) and C<sub>max</sub> were 16.71 μg.h/mL (52%) and 1363 ng/mL (40%), respectively, with a T<sub>max</sub> of 1.42 h (70%). The geometric mean of C<sub>min</sub> was 307 ng/mL (92%). Simulated t<sub>1/2 abs</sub> and t<sub>1/2 eff</sub> were 0.28 h (145%) and 12.39 h (42%), respectively. The high CVs are due to the relatively low number of patients, and the absence of samples in the absorption phase.

Additional simulations were performed to assess the impact of missed or delayed doses on belzutifan exposure. The resulting concentration-time profiles are shown in Figure S3A. Figure S3B shows the medians of all scenarios overlaid. Based on these simulations, with a single missed dose over a period of 3 days, the average daily

exposure (AUC<sub>0-24h</sub>) over a 3-day duration is reduced by 30% compared to the scenario without a missed dose (11.6 vs. 16.5 μg.h/mL). The impact of any delayed second (make up) dose on average AUC<sub>0-24h</sub> over 3 days appears small; however, C<sub>max</sub> is almost 50% higher in scenario 6 compared to q.d. dosing (scenario 1), and C<sub>min</sub> in scenario 6 is ~1/3 of the SS C<sub>min</sub> with q.d. dosing (scenario 1).

## DISCUSSION

The dose range for belzutifan was evaluated in clinical studies, and the recommended dosage is 120 mg, orally, q.d. Clinical dose ranging studies up to 240 mg q.d. did not reach a maximum tolerated dose. The recommended clinical dose of 120 mg q.d. is supported by dose ranging PK and pharmacodynamic data (dose/exposure-dependent reduction of erythropoietin with plateauing of the effect at higher dose),<sup>2</sup> efficacy and safety data from the pivotal phase II study in patients with VHL-RCC,<sup>9</sup> and extensive exposure-response analyses for efficacy and safety, which will be reported separately.

The plasma PK of belzutifan following oral administration was well-characterized by a linear two-compartment model with first-order absorption and elimination. For

**TABLE 4** Effect of UGT2B17 and CYP2C19 phenotypes on Belzutifan exposure/PK parameters.

Phenotype category	AUC <sub>ss</sub> (µg·h/mL) <sup>1</sup> (fold-change)	C <sub>max,ss</sub> (ng/mL) <sup>1</sup> (fold-change)	C <sub>min,ss</sub> (ng/mL) <sup>1</sup> (fold-change)	Clearance (L/h) <sup>1</sup> (fold-change)	Half-life (h) <sup>1</sup> (fold-change)	Arithmetic mean (range: min-max) of AUC <sub>ss</sub> <sup>2</sup>
UGT2B17 IM	19.0 (1.0×)	1483.4 (1.0×)	395.4 (1.0×)	6.3 (1.0×)	13.5 (1.0×)	Study 1: 24.2 (11.4–86.2) N = 29 Study 4: 17.9 (6.2–43.5) N = 27
UGT2B17 EM	13.7 (0.7×)	1281.6 (0.9×)	214.2 (0.5×)	8.8 (1.4×)	9.7 (0.7×)	Study 1: 13.9 (4.9–32.0) N = 28 Study 4: 13.6 (5.2–34.2) N = 25
UGT2B17 PM	27.9 (1.5×)	1909.6 (1.3×)	688.8 (1.7×)	4.8 (0.8×)	17.8 (1.3×)	Study 1: 39.5 (36.7–45.1) N = 4 Study 4: 22.7 (10.8–28.0) N = 5
UGT2B17 PM and CYP2C19 PM	43.6 (2.3×)	2539.4 (1.7×)	1305.1 (3.3×)	3.1 (0.5×)	27.8 (2.1×)	N = 0
CYP2C19 PM	29.8 (1.6×)	1904.5 (1.3×)	799.2 (2.0×)	4.0 (0.6×)	21.0 (1.6×)	Study 1: 16.1 (6.3–25.9) N = 2 Study 4: 25.6 (25.6–25.6) N = 1

*Note:* Values were obtained through univariate simulations of the same typical patient (keeping other covariates fixed and only changing UGT2B17 or CYP2C19 phenotype). Two covariates (both UGT2B17 and CYP2C19 phenotype) were changed for dual PM. Numbers in brackets are fold-change for each phenotype with respect to reference phenotype (reference typical VHL-RCC patient: age 41 years, body weight 74 kg, UGT2B17 IM, CYP2C19 non-PM, 120-mg q.d. dosing in fasted state using the FFP formulation). It is 1× for each reference value (first row). Half-life is calculated as  $\log(2) \cdot (V_2 + V_3) / CL$  (effective half-life). The last column shows calculated mean (range) of posthoc AUC<sub>ss</sub> from individual clearance and bioavailability values for patients receiving 120 mg q.d. in Studies 1 and 4. Patients in Study 1 who received a different dose were excluded. Abbreviations: AUC<sub>ss</sub>, area under the plasma concentration vs time curve at steady-state; C<sub>max,ss</sub>, maximum plasma concentration at steady-state; C<sub>min,ss</sub>, trough concentration at steady-state; EM, extensive metabolizer; IM, intermediate metabolizer; PK, pharmacokinetics; PM, poor metabolizer; q.d., once daily.

<sup>1</sup>Fold-change with respect to UGT2B17 IM.

<sup>2</sup>For 120-mg q.d. dose in Study 1 & 4 patients (classified by phenotype categories).

**TABLE 5** Derived population PK parameters for patients with VHL-RCC (120 mg q.d.).

Parameter	Formulation	Geometric mean	Geometric CV%	Arithmetic mean	Standard deviation
CL/F (L/h)	FFP, FMF	7.25	51.36	8.15	4.17
$V_d/F$ (L)	FFP, FMF	129.5	35.18	137.62	51.45
KA (1/h)	FFP	2.51	145.43	4.40	5.83
	FMF	1.32	145.43	2.32	3.06
AUC <sub>0-24h</sub> (μg·h/mL)	FFP, FMF	16.71	52.34	18.86	9.89
$C_{min}$ (ng/mL)	FFP	306.66	92.3	406.24	321.82
	FMF	318.18	91.12	418.7	326.31
$C_{max}$ (ng/mL)	FFP	1362.54	39.77	1463.81	564.83
	FMF	1263.72	42.2	1368.93	559.18
$T_{max}$ (h)	FFP	1.42	69.72	1.73	1.15
	FMF	2.05	69.56	2.48	1.57
$t_{1/2}$ alpha (h)	FFP, FMF	2.60	37.28	2.77	0.99
$t_{1/2}$ beta (h)	FFP, FMF	14.34	36.82	15.29	5.68
$t_{1/2}$ eff (h)	FFP, FMF	12.39	41.61	13.42	5.59
$t_{1/2}$ abs (h)	FFP	0.28	145.43	0.48	0.60
	FMF	0.52	145.43	0.91	1.15

*Note:* Parameters were derived by simulation of 24-h PK profiles following 120 mg q.d. administration at steady-state for either the FFP or the FMF formulation. All parameter estimates are determined under steady-state conditions. Simulated mean/median CL/F,  $V_d/F$  and KA post hoc can differ from estimated post hoc because of the small sample size ( $N=61$ ) of observations. AUC<sub>0-24h</sub>, area under the concentration vs time curve for a 24-h interval, CL, clearance; CL/F, apparent clearance;  $C_{max}$ , peak plasma concentration,  $C_{min}$ , trough concentration; CV, coefficient of variation; F, bioavailability; FFP, fit-for-purpose formulation; FMF, final market formulation; KA, absorption rate constant; PK, pharmacokinetic; q.d., once daily;  $t_{1/2}$ , terminal half-life;  $t_{1/2}$  abs, absorption terminal half-life;  $t_{1/2}$  alpha, initial elimination half-life;  $t_{1/2}$  beta, terminal elimination half-life;  $t_{1/2}$  eff, effective elimination half-life;  $T_{max}$ , time to reach maximum plasma concentration;  $V_d/F$ , apparent total volume of distribution.

patients with VHL, the mean (%CV) apparent CL and  $V_d$  were predicted to be 7.3 L/h (51%), and 130 L (35%). There were no clinically relevant differences in the PK of belzutifan based on the individual covariates of age, sex, ethnicity, race, body weight, mild/moderate renal impairment, or mild hepatic impairment. Estimated exponents for the body weight effect approximately followed the theoretical weight-based allometric scaling for clearance and volume established for typical small molecule drugs.

Food led to a reduction in KA by 88%. The FMF formulation led to a 47% lower KA. However, neither food nor formulation had any impact on AUC<sub>ss</sub>, which is the PK parameter expected to drive efficacy and safety.

The population PK analyses estimated that the UGT2B17/CYP2C19 dual PM phenotype is expected to be associated with a 3.2-fold increase in belzutifan AUC compared to UGT2B17 EM/CYP2C19 non-PMs (43.6 vs. 13.7 μg·h/mL). Of note, in the overall US population, the expected frequency of the UGT2B17/CYP2C19 dual PM phenotype is estimated at ~0.5%. In East Asians, the frequency can reach 15%.

In vitro data justify the phenotype effect for UGT2B17 and CYP2C19 on clearance. The effect of UGT phenotype on F is in line with mechanistic considerations: due to

presence of UGT, conversion of drug to metabolite takes place in the gut. It is plausible that absence of this enzyme activity, as in UGT PM patients, will lead to higher F due to less conversion to metabolite before drug absorption.

The exposure-response analyses for safety did not identify significant risk with these projected exposures (these data will be reported/published separately) in the intended clinical population, and thus, no dose adjustment is currently recommended in the approved US label.<sup>4</sup> Further data are being collected across studies to add to the information about phenotype effect, and the current labeling recommends monitoring of patients who are known to be UGT2B17/CYP2C19 dual PMs.

Simulations showed that delaying a dose up to 21 h affected the maximum and trough concentrations but had little effect on overall exposure (average AUC over 3 days). Based on these results, the labeling proposal states that if a dose of belzutifan is missed, it can be taken as soon as possible on the same day. The patient should resume the regular daily dose schedule the next day and not take extra tablets to make up for the missed dose.

In summary, based on the population PK analysis, intrinsic factors, such as age, sex, body weight/BMI, race,

ethnicity, disease status/cancer type (healthy individuals, patients with VHL-RCC, advanced RCC, or other advanced non-RCC ST), renal impairment (mild and moderate), hepatic impairment (mild impairment as categorized by NCI index), and phenotype status of any single metabolic enzyme (UGT2B17 or CYP2C19) do not have a clinically meaningful impact on belzutifan exposures (AUC), and no dose adjustment is recommended for any of these factors. These population PK-based modeling and simulation assessments provided PK parameter estimates for the relevant clinical population and for the final formulation, as well as suitable dosing recommendations for belzutifan labeling.<sup>4</sup>

## AUTHOR CONTRIBUTIONS

D.D.M., P.J., H.J.K., C.M.S., A.C., T.B., P.M.S., A.K.A., E.A.K., Y.L., R.F.P., D.P.A., and L.J. wrote the manuscript. D.D.M., C.M.S., T.B., P.M.S., A.K.A., E.A.K., Y.L., R.F.P., D.P.A., and L.J. designed the research. D.D.M. performed the research. D.D.M., P.J., and H.J.K. analyzed the data.

## ACKNOWLEDGMENTS

The authors wish to thank Phung Bondiskey, Misoo Chung Ellison, and Ananya Roy (Merck & Co., Inc., Rahway, NJ, USA) for their contributions to some of the study designs and generation of data included in this report. Medical writing support was provided by Amy C. Porter, PhD, ISMPP CMPP<sup>TM</sup> of Certara Synchrogenix, funded by Merck Sharp & Dohme LLC, a subsidiary of Merck & Co., Inc., Rahway, NJ, USA.

## FUNDING INFORMATION

This study was funded by Merck & Co. Inc.

## CONFLICT OF INTEREST STATEMENT

D.D.M. and L.J. were employees of Merck Sharp & Dohme LLC, a subsidiary of Merck & Co., Inc., Rahway, NJ, USA at the time of this work and own Merck & Co., Inc., Rahway, NJ, USA stock or stock options. P.J. and H.J.K. are employees of Certara and in that capacity are consultants for Merck & Co., Inc., Rahway, NJ, USA. C.M.S. is an employee of Merck Sharp & Dohme LLC, a subsidiary of Merck & Co., Inc., Rahway, NJ, USA, is an author of a company-owned patent, receives support for meeting attendance, and owns Merck & Co., Inc., Rahway, NJ, USA stock. A.C., E.A.K., Y.L., and R.F.P. are employees of Merck Sharp & Dohme LLC, a subsidiary of Merck & Co., Inc., Rahway, NJ, USA and own Merck & Co., Inc., Rahway, NJ, USA stock or stock options. T.B. and P.M.S. are employees of Merck Sharp & Dohme LLC, a subsidiary of Merck & Co., Inc., Rahway, NJ, USA, have patents issued or pending, receive support for travel, and own Merck & Co., Inc., Rahway, NJ, USA stock or stock options.

A.K.A. and D.P.A. were Merck Sharp & Dohme LLC, a subsidiary of Merck & Co., Inc., Rahway, NJ, USA employees at the time of this work.

## ORCID

Dhananjay D. Marathe  <https://orcid.org/0000-0003-0238-2252>

Anson K. Abraham  <https://orcid.org/0000-0002-9579-7483>

## REFERENCES

- Deeks ED. Belzutifan: first approval. *Drugs*. 2021;81:1921-1927. doi:10.1007/s40265-021-01606-x
- Choueiri TK, Bauer TM, Papadopoulos KP, et al. Inhibition of hypoxia-inducible factor-2 $\alpha$  in renal cell carcinoma with belzutifan: a phase 1 trial and biomarker analysis. *Nat Med*. 2021;27:802-805. doi:10.1038/s41591-021-01324-7
- Hasanov E, Jonasch E. Mk-6482 as a potential treatment for von Hippel-Lindau disease-associated clear cell renal cell carcinoma. *Expert Opin Investig Drugs*. 2021;30:495-504. doi:10.1080/13543784.2021.1925248
- U.S. Food and Drug Administration. Belzutifan prescribing information. 2021. Accessed August 04, 2023. [https://www.accessdata.fda.gov/drugsatfda\\_docs/label/2021/215383s000lbl.pdf](https://www.accessdata.fda.gov/drugsatfda_docs/label/2021/215383s000lbl.pdf)
- Jonsson EN, Karlsson MO. Automated covariate model building within NONMEM. *Pharm Res*. 1998;15:1463-1468. doi:10.1023/a:1011970125687
- Yafune A, Ishiguro M. Bootstrap approach for constructing confidence intervals for population pharmacokinetic parameters. I: A use of bootstrap standard error. *Stat Med*. 1999;18:581-599. doi:10.1002/(sici)1097-0258(19990315)18:5<581::aid-sim47>3.0.co;2-1
- Karlsson MO, Holford N. *A Tutorial on Visual Predictive Checks*. 2008. Accessed August 04, 2023. <https://www.page-meeting.org/?abstract=1434>
- Bergstrand M, Hooker AC, Wallin JE, Karlsson MO. Prediction-corrected visual predictive checks for diagnosing nonlinear mixed-effects models. *AAPS J*. 2011;13:143-151. doi:10.1208/s12248-011-9255-z
- Jonasch E, Donskov F, Iliopoulos O, et al. Belzutifan for renal cell carcinoma in von Hippel-Lindau disease. *N Engl J Med*. 2021;385:2036-2046. doi:10.1056/NEJMoa2103425

## SUPPORTING INFORMATION

Additional supporting information can be found online in the Supporting Information section at the end of this article.

**How to cite this article:** Marathe DD, Jauslin PM, Kleijn HJ, et al. Population pharmacokinetic analyses for belzutifan to inform dosing considerations and labeling. *CPT Pharmacometrics Syst Pharmacol*. 2023;12:1499-1510. doi:10.1002/psp4.13028